International Symposium
On Turbulence and Shear Flow
Phenomena (TSFP-9)
JUNE 30 - JULY 3, 2015 *Melbourne, Australia*

A STUDY OF THE GEOMETRICAL STATISTICS OF FLAME HOLES IN A PARTIALLY-EXTINGUISHED TURBULENT NONPREMIXED SHEAR LAYER

R. Knaus
Mechanical Science and Engineering
University of Illinois at Urbana-Champaign
1206 W. Green St.
61801, Urbana, IL
rknaus2@illinois.edu

C. Pantano
Mechanical Science and Engineering
University of Illinois at Urbana-Champaign
1206 W. Green St.
61801, Urbana, IL
cpantano@illinois.edu

ABSTRACT

We describe results of numerical simulations of turbulent nonpremixed shear layers under high-strain conditions such that flame holes are formed. The novelty of the present results resides in the use of a hydrodynamic model of flame holes, where the boundary separating burning from quenched flame regions is modeled using an edge flame closure. This removes the need for detailed transport of reactive species while incorporating the effect of extinction dynamically. A parametric study to investigate the influence of the ratio of extinction scalar dissipation to mean scalar dissipation rate and the edge flame velocity to average velocity tangential to the stoichiometric surface is presented.

1 INTRODUCTION

Turbulent diffusion flames (nonpremixed combustion) sustain a spatially continuous flame surface under sufficiently low strain conditions. At high strains, which may be localized in a flow or not, the flame can be quenched due to increased heat transfer away from the reaction zone (the quenched regions are some times called flame holes (Dold *et al.*, 1991)). Turbulent flames with extinction are relevant in modern combustors where the flame temperature is kept low to reduce pollutant formation or in lifted jet flames used for thermal protection of the burner. Here,

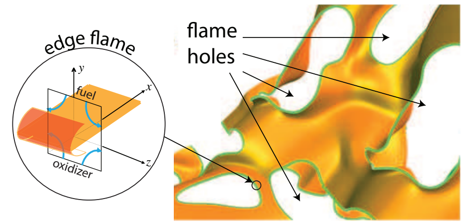

Figure 1. Flame holes in a turbulent diffusion flame (Pantano, 2004).

we are concerned with the typical combustion of hydrocarbon or hydrogen (or mixture) fuels that have thin reaction zones; analogous to simple one-step chemistry models when the activation energy is high. In this case, the reaction zone is localized (in so-called flamelets (Williams, 1975)) near the stoichiometric surface defined implicitly by $\Sigma_{\mathrm{st}} = \{x : Z(x,t) = Z_{\mathrm{st}}\}$ ($Z(x,t)$ is a conserved scalar termed the mixture fraction that takes the values of zero and one on the oxidizer and fuel streams, respectively, and Z_{st} is a constant). The magnitude of the relevant strain in a nonpremixed flame is naturally measured by the scalar rate of dissipation $\chi = 2D_{\mathrm{eff}}(\nabla Z)^2$ where D_{eff} is the effective diffusivity of the mixture fraction, approximately equal to the heat conduction coefficient of the gas. For a given fuel-oxidizer mixture, a locally thin flame can only be sustained when $\chi \lessapprox \chi_{\mathrm{q}}$, where χ_{q} is the quenching value of scalar dissipation, which is usually calculated from a simplified flame configuration such as a steady counterflow (this is why the inequality is only approximate).

When the flame is locally quenched, the nonreactive mixture cools gradually to the conditions of the free streams but a new phenomenology arises at the flame rim. The boundary that separates burning from quenched flame does not behave as a simple diffusion flame anymore. Instead, experimental and DNS data indicate that this boundary propagates with a speed that is related to χ and that the relevant combustion structure resembles closely that of an edge flame, see Fig. 1. An edge flame is a two-dimensional flame structure composed of a premixed-flame-like front (the edge) followed by a trailing diffusion flame (Buckmaster, 2002). The premixed-flame front gives this flame structure a propagating ability similar to that of pure premixed flames.

Tracking the evolution of extinction fronts in partially quenched nonpremixed flames requires following the evolution of the flame boundary. To describe this phenomenon, one could employ a complete flow-thermochemical description with hundreds of species and reaction rates, resolving all spatial and temporal scales. Since this is still too demanding for current computational resources, the alternative is to track directly the flame boundary location (as a hydrodynamic combustion model, which is a well developed technique for premixed flames). The main difficulty is that the boundary resides nominally on the moving stoichiometric surface. We are now faced with an evolution problem on a moving and shape deforming manifold embedded in the otherwise Cartesian three-dimensional space. Until very recently, there were no accurate algorithms to even simulate this problem in a computer (Kim *et al.*, 2006), let alone to study statistical properties of the flame holes or islands as a function of turbulent conditions and global combustion parameters. The most computationally tractable approach to flame hole modeling consists of recasting the evolution equation for the flame boundary (a Lagrangian description) into a level set defined on the moving stoichiometric surface (Knaus & Pantano, 2015). Then, the surface evolution equation is mapped or embedded into the three-dimensional space in order for a more standard numerical method to be applicable. The governing equation of the flame state field, φ, that indicates burning (one) or quenched (zero) states (by convention, $\varphi = 1/2$ defines the flame hole boundary itself) of the flame obeys the following equation

$$\frac{\partial \varphi}{\partial t} + \mathbf{u} \cdot \nabla \varphi = V_e(\chi)|\nabla \varphi| - \dot{Q}(\varphi, \chi), \tag{1}$$

defined only on Σ_{st}. Here, the propagation velocity of the edge flame is $V_e(\chi)$, and the quenching of the flame is described by $\dot{Q}$; both terms are obtained from canonical flame structures. The edge flame velocity has the following properties: it asymptotes to a constant value as $\chi \to 0$, there is a particular value of $\chi = \chi_0$ at which $V_e(\chi_0) = 0$ (the edge flame is stationary), and it becomes large and negative as $\chi \to \chi_q$ (we always have $\chi_0 < \chi_q$). Note that there is no need for a flame healing term since this happens naturally when two opposing boundaries of a flame hole collide and eliminate the hole. Furthermore, Eq. (1) ignores the possibility that a quenched region can be ignited by proximity of hot gases or flames, which is not expected to be very important in the conditions described in this paper. This modeling approach is termed here flame hole dynamics (FHD), a terminology due to Dold *et al.* (1991), and it is applicable when broken diffusion flames are dominant in a flow. The regions of the flame that are actively burning are typically modeled using flamelets in FHD. Therefore, one could think of FHD as a physically-based extension of flamelets to the broken flame regime.

2 QUANTITIES OF INTEREST

The development of physically sound (subgrid) models of turbulent diffusion flames experiencing extinction/reignition requires a better understanding of the statistics of quenching, i.e., the flame holes. For a given chemistry and free-stream composition, both $V_e(\chi)$ and χ_q can be approximated reasonably well by using simple canonical flame configurations (the latter defines $\dot{Q}$). But, the statistics of flame holes cannot be inferred alone from V_e and χ_q and the local and instantaneous values of χ in the flow because the quenched flame boundary has a dynamic life; rather, one must solve Eq. (1) along with the flow to determine the statistics. The purpose of the paper is to report (for the first time) results of coupled simulations where the flow is resolved completely, i.e., in a DNS sense, while the combustion is modeled hydro-dynamically using the flame hole dynamics approach.

The most fundamental question that we investigate here pertains to one-point statistics. All results are obtained from simulations of reacting temporally-evolving shear layers initialized with the fields from Pantano *et al.* (2003) for the combustion of methane with air (simulation C in that reference). The initial fields of the FHD simulations used the final fully-developed fields from that dataset where the peak Taylor microscale Reynolds number was $Re_\lambda = u'\lambda/\nu = 82$; λ denotes the Taylor microscale, u' the turbulence intensity and ν the kinematic viscosity (of the variable-density flow). The temporally evolving shear layer configuration is a good simple turbulent flow because of the presence of two homogeneous directions while nonhomogeneity exists only across the shear layer (this facilitates the calculation of accurate statistics). One drawback of the configuration is that the shear layer thickness, ℓ, grows with time. For the parameters of this study, the evolution of ℓ with time is slow in comparison with the dynamics of the flame holes, and we do not report the small growth of Reynolds number with time (the Kolmogorov scale also grows in time as $\ell^{1/4}$). Note also that the mean scalar dissipation decreases inversely proportional to ℓ.

In the flow investigated here, we have the following parameters relevant to the FHD interaction: a stoichiometric surface tangential velocity r.m.s. u'_{st}, a mean level of scalar dissipation on the surface $\bar{\chi}_{\text{st}}$, as well as its r.m.s. χ'_{st}. These are all conditioned quantities on Σ_{st}. The latter are surrogate to the normal turbulence statistics which will be denoted without the "st" subscript; in particular the Taylor microscale is expected to be of the order of the large length scales of Σ_{st}, connected with the degree of corrugation of the stoichiometric surface (a perfectly flat Σ_{st} will extinguish faster than a highly corrugated surface, given all other combustion parameters are the same, simply because there is more surface to cover). Similarly to the decrease of $\bar{\chi}$ with time, the conditional $\bar{\chi}_{\text{st}}$ also decreases with time, and its change was approximately a factor of two in the whole range of simulation time considered here. Finally, the peak u' is fixed in time (because the free-stream velocities are constant). With these parameters now defined, we can form the following nondimensional groups unique to flame hole dynamics: $\alpha = V_e(0)/u'_{\text{st}}$ (the edge flame speed relative to the level of stoichiometric turbulence) and $\beta = \chi_q/\bar{\chi}_{\text{st}}$ (extinction scalar dissipation with respect to the turbulence). In all our simulations we make the assumption that $\chi_q/\chi_0 = 3/2$. This value is not too different from what appears to happen in real hydrocarbon flames, but its effect on the evolution of the FHD statistics probably deserves careful study.

Let us define the diagnostic quantities $\mathscr{P}_q = \text{prob}_{\text{st}}(\chi > \chi_q)$, $\mathscr{P}_0 = \text{prob}_{\text{st}}(\chi > \chi_0)$ and the prognostic quantity $\mathscr{P}_h = \text{prob}_{\text{st}}(\varphi < 1/2)$, which has the property that it is zero when there is no extinction at all and one when global extinction has taken place. Note that the probabilities defined in this way are numerically equal to the ratio of the area of Σ_{st} where the condition is satisfied to the total area of Σ_{st} and also that $\mathscr{P}_0 > \mathscr{P}_q$. The questions that will be investigated here pertain to the evolution of $\mathscr{P}_q$ and $\mathscr{P}_h$ as a function of time and as a function of α and β for approximately fixed Reynolds number in a temporally evolving shear layer (Knaus & Pantano, 2009) that has been extended to the dynamically-coupled flame hole dynamics situation.

3 SIMULATION SETUP

The FHD solver utilizes a zero-Mach number formulation and solves for the pressure using a pressure-projection method within a third-order of accuracy Runge-Kutta method. Spatial discretization uses a fourth-order accurate central differencing method and boundary conditions employ the stable summation-by-parts approach of Nordstrom *et al.* (2007). The composition of the gas mixture is decomposed into burning (flame) regions of the flow, which are modeled using the Burke-Schumann approximation (infinitely-fast chemistry) for simplicity, while the quenched regions employ the mixing solution (linear in Z). These two solutions are hybridized linearly by the flame state field φ, according to

$$Y_i = (1-\varphi)Y_i^{\mathrm{m}}(Z) + \varphi Y_i^{\mathrm{f}}(Z), \tag{2}$$

$$T = (1-\varphi)T^{\mathrm{m}}(Z) + \varphi T^{\mathrm{f}}(Z), \tag{3}$$

where superscript "m" and "f" denote mixing and flame profiles, respectively (see Pantano *et al.* (2003) for the specific form of these functions). In FHD, the inner structure of the diffusion flames and of the edge flames are eliminated (by assumption) and therefore there is no need to retain more detail in the transition of Y_i and T with φ than that present in Eqs. (2)-(3). The density is then determined from the ideal gas equation of state

$$\rho = \frac{p_0}{R^0 T(Z,\varphi)} \sum \frac{Y_i(Z,\varphi)}{W_i}, \tag{4}$$

which is required to evolve the variable-density Navier-Stokes equations. Above, R^0 is the gas constant, p_0 the reference pressure (background), W_i the molecular weight of the species and N the total number of species. The temperature and composition in Eq. (4) are obtained from Eq. (3) and Eq. (2), respectively. In this study we are only concerned with combustion of methane with air, involving only the following species: CH_4, O_2, CO_2, H_2O and N_2.

A very simplistic FHD closure was employed to simplify the model to its bare-bones elements, since the focus of the paper is on the turbulence coupling and statistics (not on a quantitative predictive simulation). Therefore, the edge flame speed was modeled as

$$\frac{V_e}{V_e(0)} = 1 - \frac{1+\frac{1}{\frac{\chi}{\chi_q}-1}}{1+\frac{1}{\frac{\chi_0}{\chi_q}-1}}, \tag{5}$$

while the quenching model was taken as

$$\dot{Q}(\varphi,\chi) = R(\chi-\chi_q)\frac{2\sqrt{\varphi}}{\tau_q}, \tag{6}$$

where $R(\chi-\chi_q)$ is a ramp function,

$$R(\chi-\chi_q) = \begin{cases} 0 & \chi < \chi_q, \\ \frac{\chi-\chi_q}{\Delta_\chi} & \chi_q \le \chi < \chi_q + \Delta_\chi, \\ 1 & \chi \ge \chi_q + \Delta_\chi, \end{cases} \tag{7}$$

and Δ_χ is a parameter set to be small relative to χ_q. The time-scale τ_q denotes the characteristic time it takes for a hole to form. In this study, both $\Delta\chi$ and τ_q are kept constant and equal to $\chi_q/10$ and $0.1\ell/\Delta u$, respectively.

The fuel stream is diluted with nitrogen to a stoichiometric mixture fraction value of $Z_{\mathrm{st}} = 0.2$, which results in an adiabatic flame temperature of $T_{\mathrm{ad}} = 6.82\ T_o$, where T_o denotes the temperature of the free streams (both free streams have the same density). The simulation domain employs a uniform grid with $768 \times 258 \times 192$ points along the x, y, and z directions, respectively. The flow is homogeneous along the x and z direction (with periodic boundary conditions) and all average unconditional statistics are functions of y only. Furthermore, we assume that the diffusivity of Z and the dynamic viscosity μ are constants, independent of T, for simplicity.

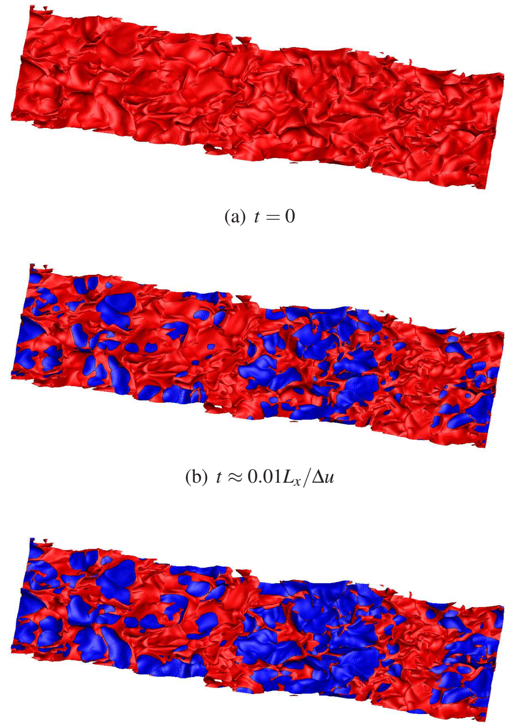

(a) $t = 0$

(b) $t \approx 0.01 L_x/\Delta u$

(c) $t \approx 0.05 L_x/\Delta u$

Figure 2. Example of flame hole formation and evolution on Σ_{st} from a shear layer DNS with stoichiometric mixture fraction $Z_{\mathrm{st}} = 0.2$.

4 RESULTS

Several instants in one of the simulations can be seen in Fig. 2, where red denotes burning flame and blue denotes extinguished regions. All the simulations are initialized with $\varphi = 1$ and are allowed to evolve in time according to the FHD closure. Holes form as soon as $\chi > \chi_q$ and grow to a size that may stabilize or quench the flame completely, depending on α and β. It is worth indicating that the asymptotic limits can be clearly identified beforehand, e.g., holes are unstable (they will always close quickly) for $\beta \to \infty$, global extinction will take place quickly for α finite and $\beta \to 0$. For other intermediate values of β, the behavior will depend on the value of $\mathscr{P}_q$ and α. For example, if the function $V_e(\chi)$ was symmetric about χ_0 one would expect that the fraction of the Σ_{st} actively burning will be very close to $\mathscr{P}_0$; but this does not happen owing to the nonlinear dependence of $V_e(\chi)$ on χ.

Table 1 list the values of the parameters α and β for all the simulations discussed here. The range of $V_e(0)/\Delta u$ ranged from 0.25 to 1, where Δu denotes the velocity dif-

Table 1. Initial parameters of the simulations.

Simulation	α	β
H1	3.333	2.45
H2	0.833	3.67
H3	1.666	3.67
H4	3.333	3.67
H5	0.833	7.35
H6	1.666	7.35

ferent of the two streams of the shear layer. In typical high-speed combustion applications, the rate limiting process is combustion and normally the proper flame velocities do not exceed the velocities in the free streams of the flow (the reason why anchoring devices – such as recirculating cavities – are needed in these applications). This explains why we focus on edge flame velocities lower than the shear layer velocity difference. Furthermore, the regime where flame holes form requires relatively low values of χ_q with respect to the χ in the flow. If χ_q is too large, there will be no extinction and no need for flame hole modeling (no broken flames). The other extreme is also uninteresting, i.e., small χ_q, because the flame ceases to exist completely.

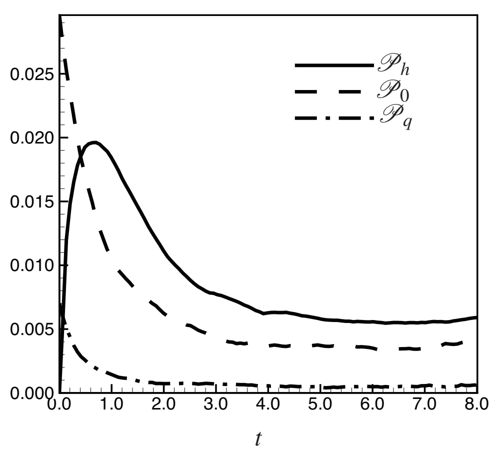

Figure 3. Evolution of the flame hole statistics as a function of time for $\alpha = 5/3$ and $\beta = 7.35$ (H6).

Figure 3 shows the evolution of $\mathscr{P}_h$, $\mathscr{P}_0$ and $\mathscr{P}_q$ as a function of time for one simulation with $\alpha = 5/3$ and $\beta = 7.35$ (simulation H6). This simulation starts with a large value of χ_q, which results in only a small fraction of Σ_{st} being quenched (peaking at about 2%). The fraction of surface for which $\chi > \chi_0$ is larger than $\mathscr{P}_q$, but overall very small, approximately 3%. Initially, the fraction of actually extinguished flame surface, measured by $\mathscr{P}_h$, grows but remains bounded between $\mathscr{P}_0$ and $\mathscr{P}_q$. But, because of the nonlinearity of the FHD, eventually, the fraction of extinguished flame exceeds $\mathscr{P}_0$ because once a hole is formed, it can only close at a maximum speed that is bounded by $V_e(0)$, contrary to extinction, which takes place over a much smaller timescale on whatever spatial extent where $\chi > \chi_q$. After the initial transient, a quasi-stationary behavior appears to settle in the simulation. The probabilities (or area fractions) do not approach a constant value because $\tilde{\chi}_{\text{st}}$ keeps decreasing but if we were to normalize $\mathscr{P}_h$ and $\mathscr{P}_0$ by $\mathscr{P}_q$, we will recover the results in Figure 4. As can be seen in the figure, for the parameters of this simulation, the amount of actual extinction can be an order of magnitude larger than $\mathscr{P}_q$ and it is always larger than $\mathscr{P}_0$ after the initial transient (this transient being artificial due to our initialization choice).

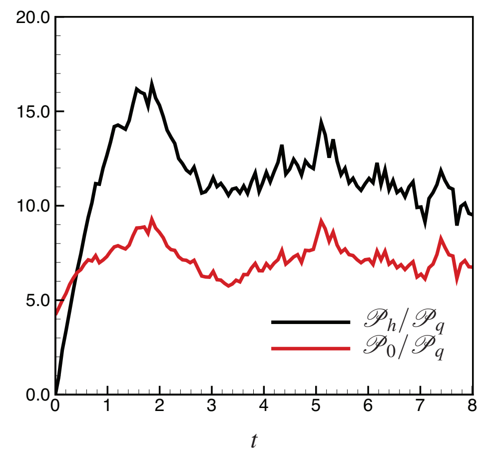

Figure 4. Normalized extinction probabilities for simulation H6 as a function of time.

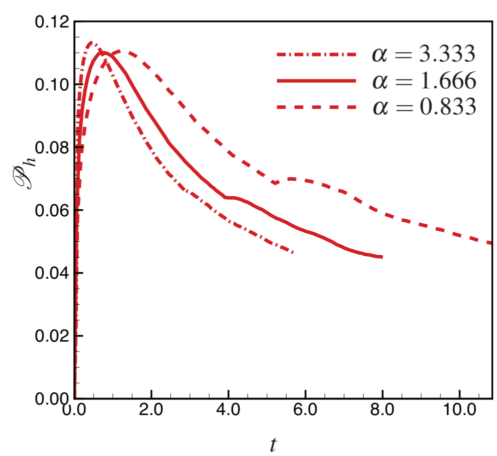

Figure 5. Fraction of Σ_{st} extinguished, $\mathscr{P}_h$, for simulations H2 to H4 as a function of time.

Figure 5 shows $\mathscr{P}_h$ for simulations H2, H3 and H4 where the initial value of χ_q was half of that in the previous figures. Now, there is as much as 10% extinction in the flame, which decreases in time due to the decrease in $\tilde{\chi}_{\text{st}}$ with time, as discussed previously. This figure explores the effect of various $V_e(0)$, parameterized by α, and shows that the flame heals faster as α increases, consistent with expectation. The effect of α on the magnitude of $\mathscr{P}_h$ is much smaller than that of β (halving β increases extinction by a factor of 5). Figure 6 shows this latter effect where for $\beta = 2.45$ almost 18% of the flame extinguishes (peak), and we also observe that the overall extinction rate decreases very fast with increasing β.

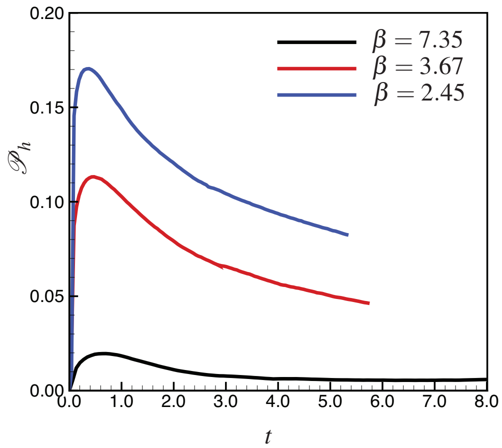

Figure 6. Effect of β on the total extinction probabilities for simulations H1, H4, and H6.

To conclude this investigation we also compared results with simulations where the density was kept constant equal to the free stream value. These cold simulations were carried out to exhibit the opposite effect observed in the variable-density simulations described previously. When we fix the density to a constant value, the flow has suddenly a higher Reynolds number (locally interpreted) and the area of Σ_{st} increases with time as well as the average value of $\bar{\chi}_{\mathrm{st}}$. This models a situations where a flame maybe passing through a contraction or compression and locally experiencing higher Reynolds numbers. These effects of changing the intensity of turbulence can be seen in Figure 7, as both black curves grow in time. Eventually, beyond the times simulated here, they will start to decay in time as the reactive simulation does, but this was not pursued here because the interest was in the increasing scalar dissipation case.

The effect of increasing magnitude of $\bar{\chi}_{\mathrm{st}}$ can be seen in Figure 8. Now, the rate of extinction keeps increasing with time (reaching up to 35% in one case for the time interval considered) due to the generation of smaller scales produced by the sudden change in density in the flow.

5 CONCLUSIONS

We have conducted a new kind of turbulent combustion simulation where the fluid dynamics is solved accurately while the combustion fields, composition and temperature, are modeled using a hydrodynamic theory of broken flames known as flame hole dynamics. This modeling approach applies to diffusion flames experiencing sufficiently high rates of strain that some of the flame surface is quenched. The advantage of this technique is that there is no need to resolve the thin (and demanding) inner structure of a flame. At the

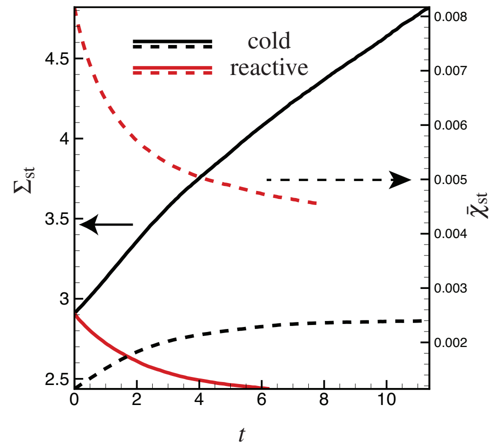

Figure 7. Variation of total area of stoichiometric surface (continuous line) and average scalar dissipation (broken line) as a function of time in variable density (reactive) and constant density (cold) simulations.

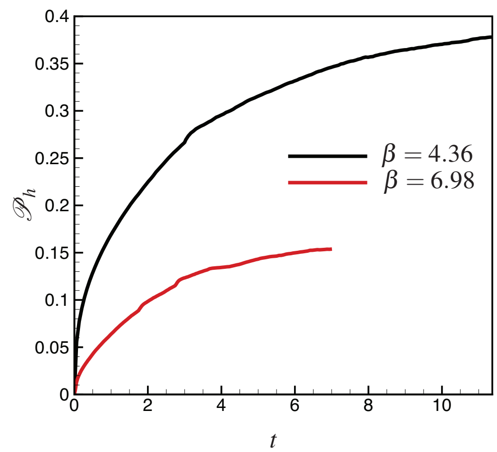

Figure 8. Extinction rate for cold simulations where $\alpha = 1.66$ and two values of β.

boundary separating quenched from burning flame regions it is postulated (supported by existing evidence) that edge flames are a reasonable description of the micro-combustion processes taking place. Then, we solve directly the flame hole dynamics equations on the moving stoichiometric surface as the flow evolves. The fluid is affected by combustion since the density is inferred from the ideal gas equation of state that employs the composition of the gas mixture deduced from the combustion closure.

The results of simulations using reacting temporally evolving shear layers show that the extension of flame holes is larger than the area of the stoichiometric surface where the instantaneous extinction criteria is satisfied. This happens because flame holes, once formed, can keep growing in size due to the negative propagation of the flame boundary velocity, even to regions where the scalar dissipation is lower than the quenching value. We explore several initial conditions to highlight the effect of the relative value of quenching value of scalar dissipation to the mean value on the stoichiometric surface and it is found that this is the dominant parameter controlling extinction. The actual level of extinction can be up to an order of magnitude higher (for our simulations, at our Reynolds number) than the fraction of stoichiometric surface experiencing local quenching conditions. The impact of the asymptotic value of the edge flame velocity is minor.

This work was supported in part by a grant from NSF CBET #1236164.

REFERENCES

Buckmaster, J. 2002 Edge-flames. *Progress in Energy and Combustion Science* **28** (5), 435–475.

Dold, J.W., Hartley, L.J. & Green, D. 1991 Dynamics of laminar triple-flamelet structures in non-premixed turbulent combustion. In *Dynamical Issues in Combustion Theory*. The IMA Volumes in Mathematics and its Applications.

Kim, J., Chung, S.H., Ahn, K.Y. & Kim, J.S. 2006 Simulation of a diffusion flame in turbulent mixing layer by the flame hole dynamics model with level-set method. *Combustion Theory and Modelling* **10** (2), 219–240.

Knaus, R. & Pantano, C. 2009 On the effect of heat release in turbulence spectra of non-premixed reacting shear layers. *Journal of Fluid Mechanics* **626**, 67.

Knaus, R. & Pantano, C. 2015 A computational approach to flame hole dynamics using an embedded manifold approach. *Journal of Computational Physics* **under review**.

Nordstrom, J., Mattsson, K. & Swanson, C. 2007 Boundary conditions for a divergence free velocity-pressure formulation of the Navier-Stokes equations. *J. Comput. Phys.* **225** (1), 874–890.

Pantano, C. 2004 Direct simulation of non-premixed flame extinction in a methane-air jet with reduced chemistry. *J. Fluid Mech.* **514**, 231–270.

Pantano, C., Sarkar, S. & Williams, F.A. 2003 Mixing of a conserved scalar in a turbulent reacting shear layer. *Journal of Fluid Mechanics* **481**, 291–328.

Williams, F. A. 1975 Recent advances in theoretical descriptions of turbulent diffusion flames. In *Turbulent Mixing in Non-reactive and Reactive Flows*. Plenum, New York.